

Synthesis, Computational Docking Study, and Biological Evaluation of a Library of Heterocyclic Curcuminoids with Remarkable Antitumor Activity

Kenneth K. Laali,^{*[a]} William J. Greves,^[a] Angela T. Zwarycz,^[a] Sebastian J. Correa Smits,^[a] Frederick J. Troendle,^[a] Gabriela L. Borosky,^[b] Sharoon Akhtar,^[c] Alak Manna,^[c] Aneel Paulus,^[c, d] Asher Chanan-Khan,^[d] Manabu Nukaya,^[e] and Gregory D. Kennedy^[e]

In a continuing search for curcuminoid (CUR) compounds with antitumor activity, a novel series of heterocyclic CUR–BF₂ adducts and CUR compounds based on indole, benzothiophene, and benzofuran along with their aryl pyrazoles were synthesized. Computational docking studies were performed to compare binding efficiency to target proteins involved in specific cancers, namely HER2, proteasome, VEGFR, BRAF, and Bcl-2, versus known inhibitor drugs. The majority presented very good binding affinities, similar to, and even more favorable than those of known inhibitors. The indole-based CUR–BF₂ and

CUR compounds and their bis-thiocyanato derivatives exhibited high anti-proliferative and apoptotic activity by in vitro bioassays against a panel of 60 cancer cell lines, more specifically against multiple myeloma (MM) cell lines (KMS11, MM1.S, and RPMI-8226) with significantly lower IC₅₀ values versus healthy PBMC cells; they also exhibited higher anti-proliferative activity in human colorectal cancer cells (HCT116, HT29, DLD-1, RKO, SW837, and Caco2) than the parent curcumin, while showing notably lower cytotoxicity in normal colon cells (CCD112CoN and CCD841CoN).

Introduction

Parent curcumin **1** (Figure 1) is a nontoxic phenolic natural product. The central core of **1** is a conjugated β -keto-enolic moiety that can participate in hydrogen bonding, act as Michael acceptor, and coordinate to metal ions, while its hydrophobic phenyl domains are potential sites for π – π interactions with the aromatic side chains in amino acids, and the phenolic hydroxy groups are capable of hydrogen bonding interactions.^[1]

The combination of these structural features and its ability to influence multiple signaling molecules have made it very challenging to unravel the biological profile of curcuminoids

(CUR) and to identify its pharmacophore, despite extensive studies aimed at improving its pharmacokinetic profile and potency.^[2–4] Whereas the potential health benefits of **1** and its anticancer, anti-inflammatory, antioxidant, and anti-mutagenic effects have been extensively studied and documented,^[5] unfavorable bio-physicochemical features, namely poor solubility, low absorption, low bioavailability, and rapid metabolism, have thus far prevented the development of a CUR-based anticancer drug.

To address these shortcomings, extensive research has focused on the synthesis of structurally modified CURs. These include changes in aryl substitution patterns, synthesis of unsymmetrical CUR compounds by introducing two different aryl groups, introduction of diverse substituents at the central methylene carbon atom, as well as more drastic structural modifications such as converting the 1,3-diketone moiety into prazoles and isoxazoles, or complete deconstruction to monocarbonyl derivatives in order to prepare CUR mimics. These highly diverse structural modifications and their biological activity outcomes were summarized in a 2014 review.^[3] Considering drug delivery aspects, encapsulation into water-soluble hosts, conjugation with nanoparticles, polymeric micelles, or liposomes have been explored as possible methods to deliver curcumin to cancer cells.^[6]

With the goal to use selective fluorine introduction as a strategy to increase metabolic stability, in an earlier study we reported the synthesis, computational docking, and in vitro bioassay studies of a library of “CUR-inspired” compounds bearing fluorinated moieties, using practical methods for selec-

[a] Prof. K. K. Laali, W. J. Greves, A. T. Zwarycz, S. J. Correa Smits, Dr. F. J. Troendle
Department of Chemistry, University of North Florida, 1 UNF Drive, Jacksonville, FL 32224 (USA)
E-mail: kenneth.laali@unf.edu

[b] Dr. G. L. Borosky
INFIQC, CONICET and Departamento de Química Teórica y Computacional, Facultad de Ciencias Químicas, Universidad Nacional de Córdoba, Ciudad Universitaria, Córdoba 5000 (Argentina)

[c] S. Akhtar, Dr. A. Manna, Dr. A. Paulus
Department of Cancer Biology, Mayo Clinic, Jacksonville, FL (USA)

[d] Dr. A. Paulus, Dr. A. Chanan-Khan
Department of Hematology and Oncology, Mayo Clinic, Jacksonville, FL (USA)

[e] Dr. M. Nukaya, Prof. G. D. Kennedy
Department of Surgery, University of Alabama–Birmingham School of Medicine, Birmingham AL 35294-0016 (USA)

Supporting information and the ORCID identification number(s) for the author(s) of this article can be found under:
<https://doi.org/10.1002/cmdc.201800320>

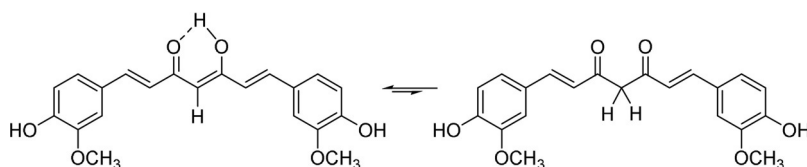


Figure 1. Tautomerism in **1**—exclusive presence of the enol tautomer.

tive fluorine introduction into the α -carbonyl moiety.^[7] Our subsequent study focused on the synthesis of a library of CUR–BF₂ adducts and CURs with diverse substitution patterns in the phenyl rings.^[8] To that end, fluorinated substituents (SCF₃, OCF₃, and F) were introduced in an effort to improve lipophilicity and metabolic stability, whereas bulky activating groups (OMe, OAc, and OBz) were introduced as a way to tune steric and electronic effects.^[8] To gauge the potential role of the enolic moiety in interaction with proteins, a library of fluorinated aryl pyrazoles and isoxazoles were also synthesized and characterized.^[8]

Studies of heterocyclic curcuminoids have so far focused mainly on systems in which the diketo linker has been replaced with piperid-4-one, tetrahydrothiopyran-4-one, or tetrahydropyran-4-one moieties. There are also limited examples in which phenyl rings were replaced with thiophene, pyrrole, or pyridine, while maintaining the 1,3-keto-enolic structural motif. Synthetic progress along with the pharmacological properties of these compounds have been reviewed.^[9]

Herein we report the synthesis of a library of heterocyclic CUR–BF₂ and CUR compounds based on indole, benzothio- phene, and benzofuran, including several examples of their aryl pyrazole derivatives. We also report computational/dock-

ing studies and bioassays of this class of compounds focusing on multiple myeloma and colorectal cancer.

Results and Discussion

Our earlier reported one-pot method for the synthesis of CUR–BF₂ adducts^[7,8] was used in the present study for the synthesis of heterocyclic analogues starting with the corresponding aldehydes. In the majority of cases, the CUR–BF₂ adducts precipitated from ethyl acetate after overnight stirring at room temperature as detailed below.

Synthesis

Synthesis of indole-based CUR–BF₂ adducts and CUR compounds

a) From indole 5-aldehyde: The initial crop that precipitated out of ethyl acetate was a tautomeric mixture of **2a**–BF₂ and **2**–BF₂ in 60:40 ratio as determined by NMR spectroscopy (Figure 2A). By adding more base to the filtrate and continuing stirring overnight, a second crop was produced that proved to be the enolic tautomer **2**–BF₂. In independent runs **2**–BF₂ was

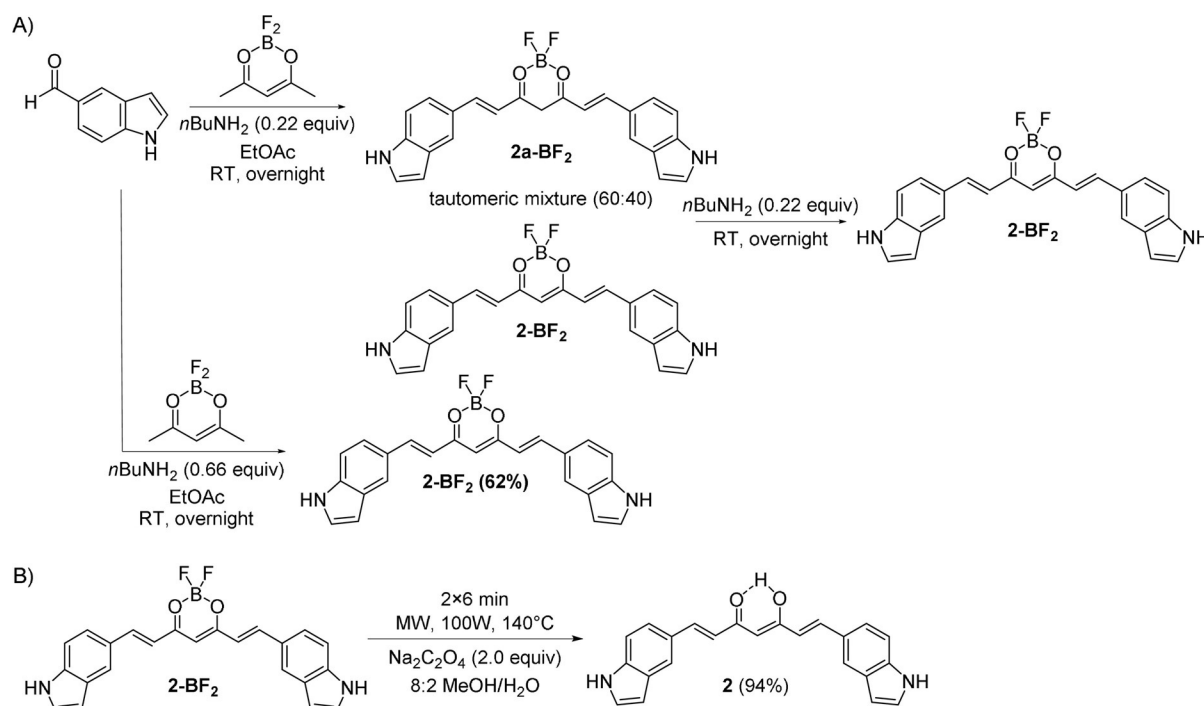


Figure 2. A) CUR–BF₂ adducts from indole-5-aldehyde; B) Microwave-assisted synthesis of curcuminoid **2**.

isolated as the sole product by using 0.66 equivalents of base after overnight stirring.

When a portion of crop 1 (CUR-BF₂ tautomeric mixture) was subjected to microwave (MW)-assisted decomplexation, a tautomeric mixture of the corresponding CURs **2a** and **2** were obtained with the enolic tautomer **2** predominating. Decomplexation of another portion of the tautomeric mixture similarly resulted in a tautomeric mixture in which **2** was the major product. Finally, MW-assisted decomplexation of **2-BF₂** furnished compound **2** purely as the enol tautomer in 94% isolated yield (Figure 2).

b) From indole 4-aldehyde: In initial studies (on a 500 mg scale), no precipitate was formed after three days mixing at room temperature. Removal of ethyl acetate gave a dark residue, which, after washing with diethyl ether, was shown by NMR to be a tautomeric mixture of enolic and the diketo forms in 4:1 ratio. By addition of more base and by using less ethyl acetate in a subsequent reaction, **3-BF₂** precipitated solely as the enol tautomer. MW-assisted decomplexation cleanly gave the corresponding curcuminoid **3** as an enolic compound in 77% isolated yield (Figure 3).

c) Synthesis of bis-thiocyanato derivatives of indole-based CUR-BF₂ and CUR compounds: There is currently considerable interest in the introduction of thiocyno groups into bioactive compounds,^[10] and this, in turn, has stimulated a search for new thiocyanation methods.^[11] Development of a new method in our research group for the facile introduction of SCN and SeCN groups into medicinally important heterocycles^[12] has enabled the synthesis of bis-thiocyanato CUR-BF₂ and CUR compounds starting from the SCN-substituted benzaldehydes (Figure 4).

Because attempts to obtain X-ray-quality crystals from the CUR-BF₂ or CUR compounds in this class were not successful,

their structures were optimized by density functional theory (DFT) calculations. Two representative examples (**4-BF₂** and **5-BF₂**) are shown in Figure 5, while other examples are gathered in the Supporting Information (Figure S1).

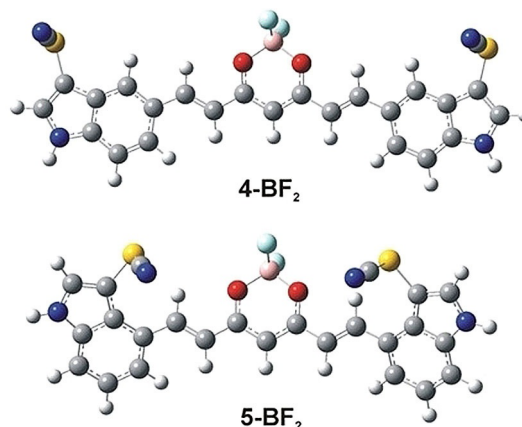


Figure 5. Structures of **4-BF₂** and **5-BF₂** optimized at the B3LYP/6-31G(d) level.

d) From *N*-methylindole-3-aldehyde: Following our standard protocol, in a small-scale experiment *N*-methylindole-5-carboxaldehyde reacted to give the 1,3-diketo tautomer **6a-BF₂** as a deep-purple solid, which was harvested in two crops in 22% combined yield (Figure 6). The MW-assisted decomplexation of **6a-BF₂** cleanly furnished the corresponding curcuminoid **6a** solely as the 1,3-diketo tautomer in 64% isolated yield.

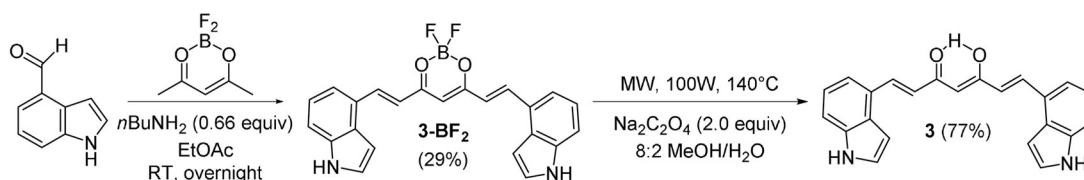


Figure 3. Synthesis of **3-BF₂** and **3** from indole-4-aldehyde.

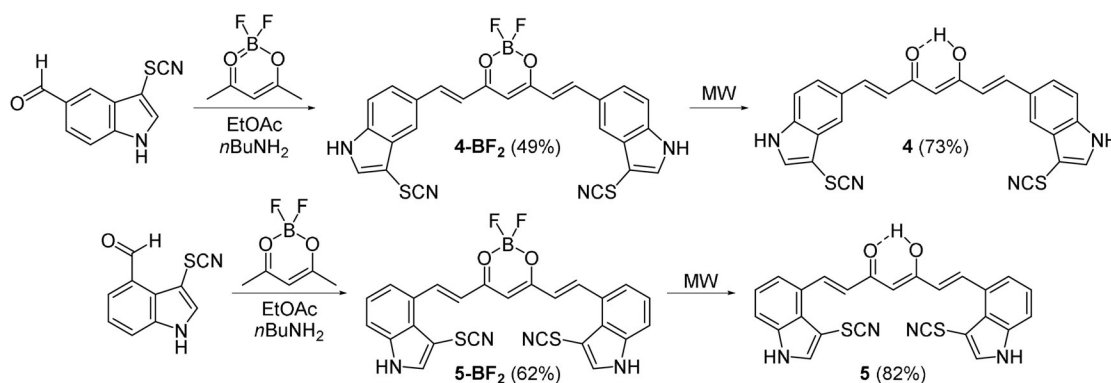


Figure 4. Synthesis of bis-thiocyanato CUR-BF₂ and CUR compounds.

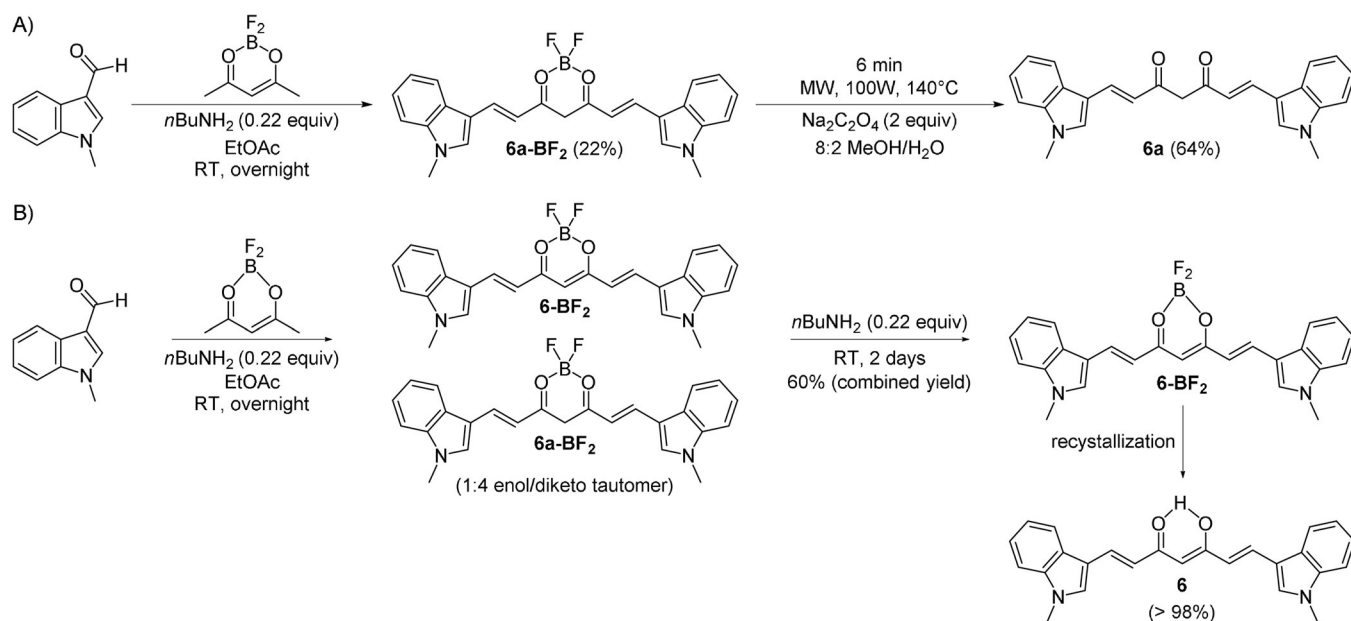


Figure 6. A) Isolation of **6a-BF₂** and its decomplexation to **6a**; B) Synthesis of **6-BF₂**/**6a-BF₂** and decomplexation to **6**.

A second synthesis (Figure 6B) using less ethyl acetate produced two crops: the first crop precipitated overnight (a red solid) as a 4:1 tautomeric mixture, and the second crop was harvested after the addition of more base to the filtrate and stirring at room temperature for two days; this was solely the enolic **6-BF₂** (a green solid). Decomplexation of **6-BF₂** required multiple runs in the microwave followed by re-crystallization from methanol to cleanly furnish compound **6** as a bright-red solid (Figure 6B).

Synthesis of heterocyclic benzothiophene- and benzofuran-based CUR-BF₂ and CUR compounds and their aryl pyrazoles

Following our general one-pot method described earlier,^[8] the corresponding CUR-BF₂ adducts and CUR compounds in Figure 7 were synthesized by starting from the corresponding aldehydes. NMR spectra confirmed the sole presence of the enolic tautomers in every case.

With the goal to determine the significance of the keto-enolic moiety in bioactivity for this class of compounds, a

small library of aryl pyrazoles **10–15** were also synthesized (Figure 8) following our earlier reported method.^[8]

Computational docking studies

Molecular docking calculations were carried out with the aim to shed light on factors that govern the biological activity of the heterocyclic curcuminoids. Binding affinities in the active site of various proteins involved in carcinogenic mechanisms were determined, and computed binding energies were compared with those of the corresponding known inhibitors (Table 1). The proteins selected for docking studies comprise a variety of oncogenic processes, described as follows.

Human epidermal growth factor receptor 2 (HER2), which is one of the tyrosine kinase receptors in the epidermal growth factor receptor (EGFR) family, plays a crucial role in the evolution of several human cancers.^[13] It is a target for therapies pointing to inhibition of HER2 to decrease tumor growth, as amplification or overexpression of this protein appears in breast, prostate, gastric/gastroesophageal, ovarian, endometrial, bladder, lung, colon, and head and neck cancers.^[13] It has

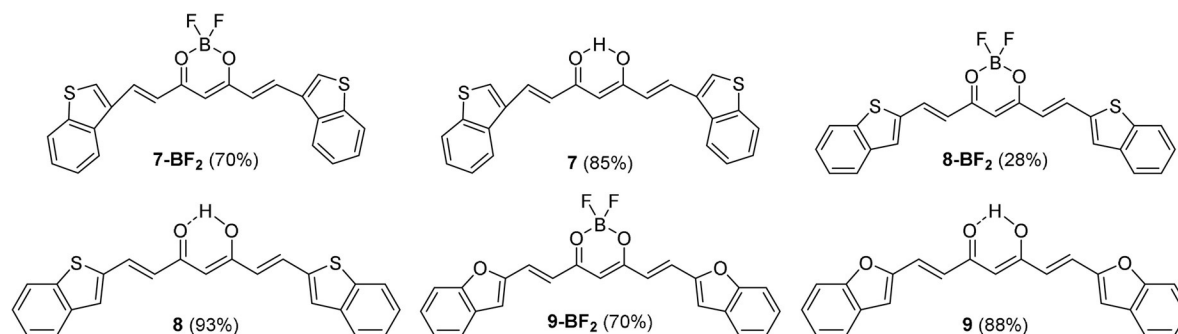


Figure 7. Heterocyclic CUR-BF₂ and CUR based on benzothiophene and benzofuran.

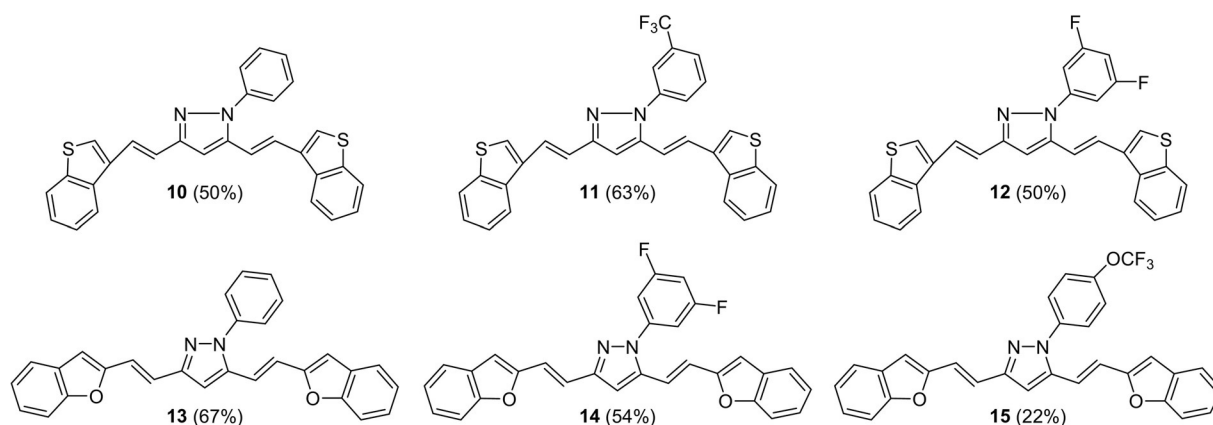


Figure 8. Heterocyclic CUR-aryl pyrazoles based on benzothiophene and benzofuran.

been suggested that inhibition of the tumor cell proteasome is the mechanism by which curcumin prevents the proliferation of acute promyelocytic leukemia (APL) cells.^[14] Treatment with proteasome inhibitors causes a decrease in proliferation, induction of apoptosis, and sensitization of diverse tumor cells to chemotherapeutic drugs and irradiation.^[15] The vascular endothelial growth factor receptor (VEGFR) tyrosine kinases are clinically confirmed targets of inhibitors applied in renal cell carcinoma therapy.^[16] The treatment of metastatic melanoma significantly evolved by selective inhibition of BRAF, as oncogenic activation of this protein stimulates cancer cell growth.^[17] The connection of proteins in the Bcl-2 family (crucial regulators of normal apoptosis) with tumor initiation, disease progression, and drug resistance makes them crucial targets for antitumor therapy.^[18] Bcl-2 is overexpressed in acute and chronic leukemias and plays a central role in the survival of multiple lymphoid malignancies.^[18] The studied CUR-BF₂ and CUR compounds were able to fit nicely into the binding pockets of the considered proteins, and several compounds revealed markedly favorable binding affinities (Table 1). In proteasome, VEGFR, and Bcl-2, several CUR derivatives presented enhanced binding energies in comparison with known inhibitors that are used in chemotherapy. Notably, the docking energy for the 1,3-diketo tautomer (as in **2aBF₂**) is also predicted to be highly favorable, suggesting that in the case of tautomeric mixtures both tautomers are capable of favorable docking interactions. Binding interactions for the compounds exhibiting highly favorable docking energies in the active site of each protein are displayed in Figure 9.

The principal interactions observed are hydrophobic contacts between the atoms of the ligands and the protein residues (red radial lines). In addition, hydrogen bond interactions were found between F and N ligand atoms and hydrogen bond donor groups in neighboring protein residues. Figure 10 depicts a 3D representation of **3-BF₂** in Bcl-2.

In vitro bioassays

The heterocyclic CUR-BF₂ and CUR compounds synthesized in the present study along with representative aryl pyrazoles were initially tested for their anti-proliferative activity in the US

National Cancer Institute 60-cell-line (NCI-60) in vitro assay panel. Among these, the indole-based CUR-BF₂ and CUR compounds, and in particular their bis-thiocyanato derivatives (Figure 11), exhibited notable anti-proliferative and apoptotic activity in a number of cell lines in several types of cancers, as reflected in either low or negative growth percentage values, respectively, under the standard concentration of 10⁻⁵ M (Supporting Information (SI) Figures S1–S6). Subsequent five-dose assay on these compounds (performed at the NCI) showed significant anti-proliferative activity remaining at 10⁻⁶ M, followed by a rapid drop at lower concentrations. Among the *N*-methylindole derivatives and the benzothiophene- and benzofuran-derived CUR-BF₂ and CUR compounds, only **7-BF₂** showed notable anti-proliferative activity (SI Figure S7), while the corresponding aryl pyrazoles proved to be ineffective.

Compounds shown in Figure 11 were subsequently tested to determine their ability to induce cytotoxicity in a small panel of hematologic cancer cell lines in comparison with healthy (noncancer) peripheral blood mononuclear cells (PBMCs). The indole-CUR and CUR-BF₂ compounds exhibited significant cytotoxicity in multiple myeloma (MM) cancer cells, with little to no cell death noted in healthy donor PBMCs.

Further bioassay studies focused on an expanded panel of MM cell lines that capture some of the genetic variability observed in MM patients. Notably, these MM cell lines included MM1.S cells (*TP53* wild-type), KMS11 cells (*TP53* biallelic deletion) and RPMI-8226 cells (*c-Myc* dependent). Among these select groups of heterocyclic curcuminoids, **3-BF₂** and **2** exhibited remarkable tumor-selective activity, with median IC₅₀ values in the aforementioned MM cell lines of 2.1 μM and 1.4 μM, respectively (Table 2). They also showed notable MM-cell-specific cytotoxicity, with mean activity of 33.7-fold (range: 4- to 2445-fold) greater in the MM cell lines relative to healthy PBMCs (Figure 12 and Table 3). Notably, the MM standard-of-care agent bortezomib (a proteasome inhibitor) has an in vitro tumor specificity profile of roughly 2- to 3-fold (IC₅₀ in MM cells ≈ 2 nM and IC₅₀ of PBMCs is ≈ 4–6 nM).

Next, the ability of these hit compounds to induce apoptotic cell death was assessed by annexin-V/PI staining (Figure S8). With **3-BF₂**, significant apoptosis in MM1.S (34% and 47%), KMS-11 (75% and 79%), and RPMI-8226 (39% and 60%) cells

Table 1. Calculated binding energies for heterocyclic curcuminoids versus known inhibitors.

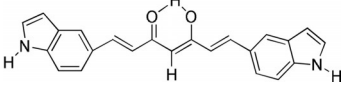
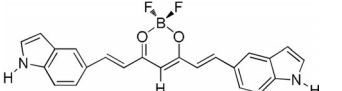
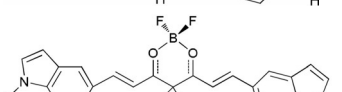
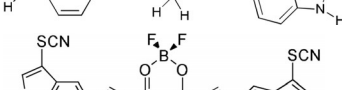
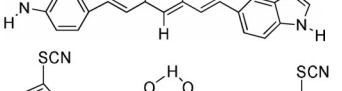
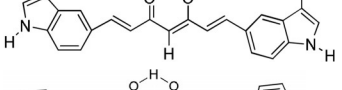
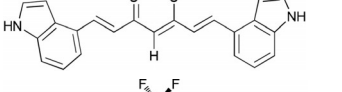
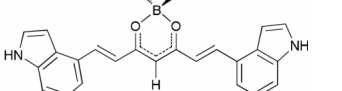
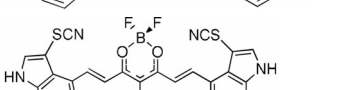
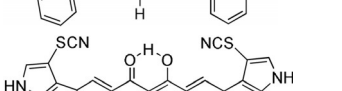
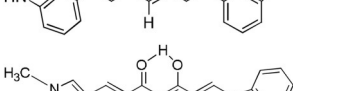
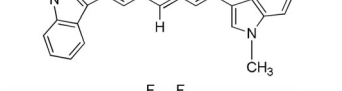
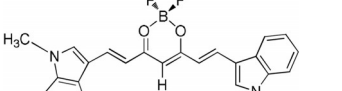
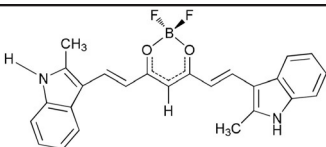
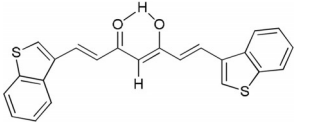
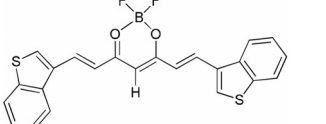
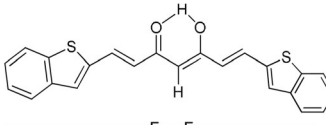
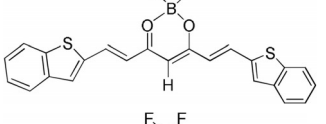
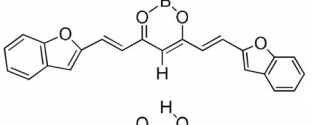
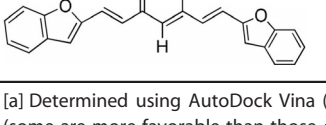
Compound	HER2	Proteasome	E_{bind} [kcal mol ⁻¹] ^[a] VEGFR	BRAF	Bcl-2
Known inhibitors	-11.4 (SYR)	-7.8 (bortezomib)	-9.2 (axitinib)	-9.3 (vemurafenib)	-8.3 (navitoclax)
		-7.8 (ixazomib)	-10.8 (sorafenib)	-12.9 (dabrafenib)	-8.2 (venetoclax)
		-8.5 (carfilzomib)	-8.9 (lenvatinib)		
	-11.0	-9.6	-11.7	-10.2	-8.6
	-10.8	-10.4	-12.6	-10.6	-8.7
	-10.5	-10.3	-12.5	-10.7	-9.4
	-10.4	-9.9	-12.4	-10.9	-8.3
	-8.9	-10.1	-11.5	-9.8	-9.4
	-10.1	-9.6	-10.5	-10.2	-7.7
	-10.2	-10.5	-11.7	-10.3	-9.4
	-9.3	-10.8	-10.0	-10.1	-7.7
	-8.7	-9.4	-9.4	-9.2	-6.6
	-9.0	-9.6	-9.9	-9.5	-9.3
	-9.4	-10.1	-11.2	-10.2	-9.2
	-9.6	-10.5	-11.8	-10.7	-8.5
	-10.2	-9.4	-10.8	-10.9	-9.0

Table 1. (Continued)

Compound	E_{bind} [kcal mol ⁻¹] ^[a]				
	HER2	Proteasome	VEGFR	BRAF	Bcl-2
	-11.7	-10.5	-11.4	-11.1	-8.7
	-9.8	-9.3	-10.4	-9.6	-8.8
	-10.5	-9.9	-11.1	-10.4	-8.5
	-9.8	-8.9	-11.2	-9.5	-8.0
	-10.7	-9.1	-12.7	-10.8	-7.7
	-11.6	-10.0	-13.3	-11.0	-8.0
	-9.9	-9.9	-11.7	-10.1	-8.2

[a] Determined using AutoDock Vina (version 1.1.2); values are from the most stable binding mode. Highly favorable binding energies are shown in bold (some are more favorable than those of known inhibitors).

was noted relative to healthy donor PBMCs, treated with the same concentrations (1.25 μM and 2.5 μM , 24 h exposure; 23–28% apoptosis observed). Next, the MM cells and PBMCs were tested with CUR-analogue **2**, showing that in line with cell proliferation assay data (Figure 12), RPMI-8226 cells were most sensitive to this compound with 32% and 65% of cells undergoing apoptosis at 1.25 μM and 2.5 μM concentrations, respectively. In contrast, in KMS11 and MM1.S cells, notable apoptosis (54% and 15%, respectively) was observed only at a concentration of 10 μM . For comparison, the same MM cell lines were exposed to venetoclax (USFDA-approved anti-Bcl-2 inhibitor, activator of apoptosis) at concentrations of 1.25, 2.5, 5, and 10 μM , showing a median apoptosis of 15%, with \approx 10% cell death seen in healthy donor PBMCs (Figure S8).

Compounds shown in Figure 11 along with two other CUR-BF₂ compounds from our earlier study^[8] (SI Figure S9) were subsequently tested for their anti-proliferative activity in colorectal cancer (CRC) cells and in normal colon cells (SI Figure S10) in comparison with parent curcumin. The CUR-BF₂ adducts and in particular, the bis-SCN derivatives, exhibited significantly higher anticancer activity (growth inhibition) than

curcumin, whereas the corresponding CUR compounds were less effective. Moreover, relative to parent curcumin, the CUR-BF₂ adducts were notably more toxic to cancer cells than to normal colon cells (Figure 13 and Figure S11).

Conclusions

In the present study a series of new heterocyclic CUR-BF₂ and CUR compounds based on indole, benzothienopyridine, and benzofuran were synthesized and characterized. Whereas computational docking studies showed that a fairly large subset of these compounds are capable of favorable docking interactions with several key proteins involved in carcinogenic mechanisms, bioassay studies pointed to a smaller subset and in particular two curcuminoids (**3-BF₂** and **2**) with favorable cytotoxicity characteristics as potential hit compounds. Guided by the initial NCI-60 data, the anti-proliferative and apoptotic efficacy of the CUR-BF₂ and CUR compounds (SI Figure S9) were studied in colorectal cancer (CRC) cells. The CUR-BF₂ adducts, and in particular the bis-SCN derivatives, exhibited significantly higher anticancer activity than curcumin. Moreover, these com-

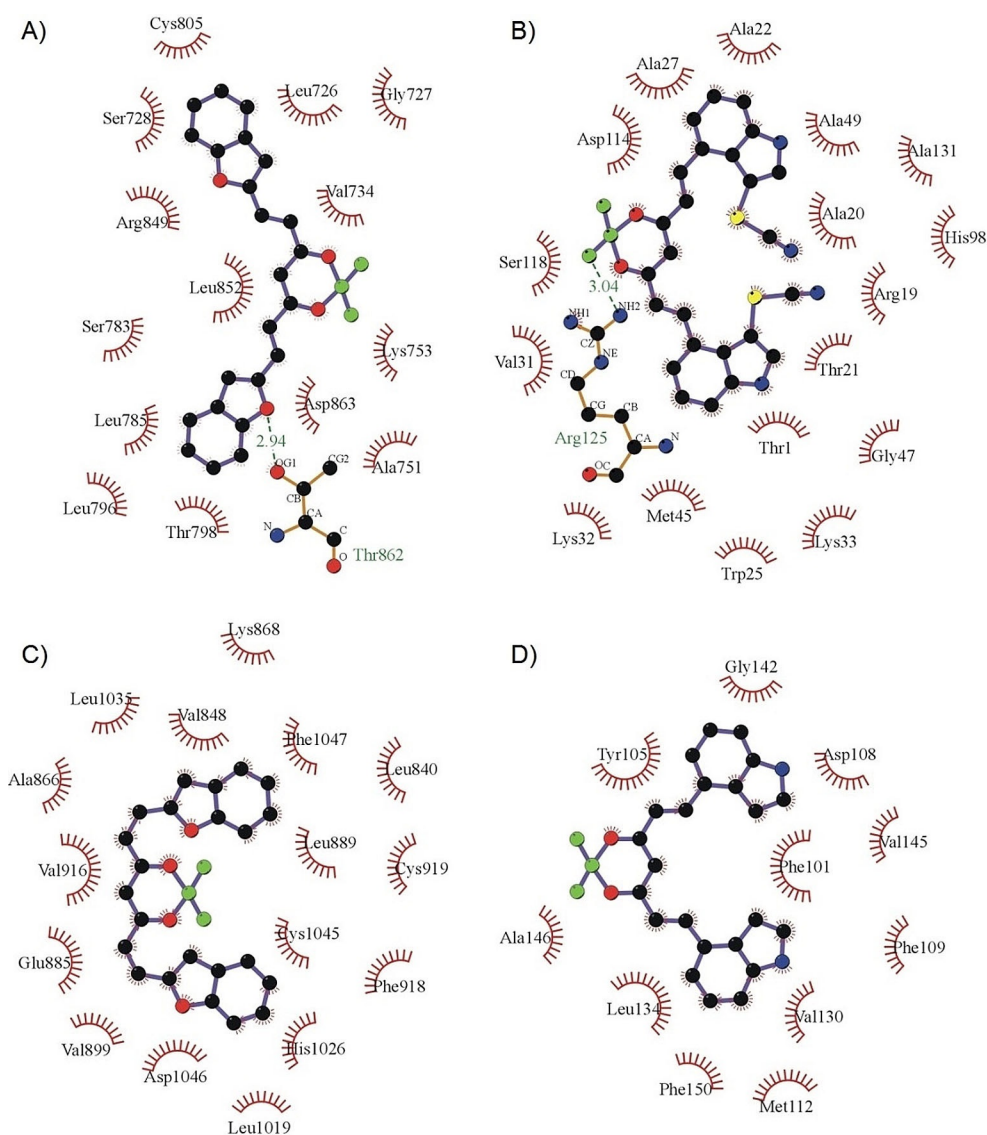


Figure 9. Most favorable binding interactions in the active sites of the studied enzymes. A) 9-BF₂ in HER2; B) 5-BF₂ in proteasome; C) 9-BF₂ in VEGFR2; D) 3-BF₂ in Bcl-2.

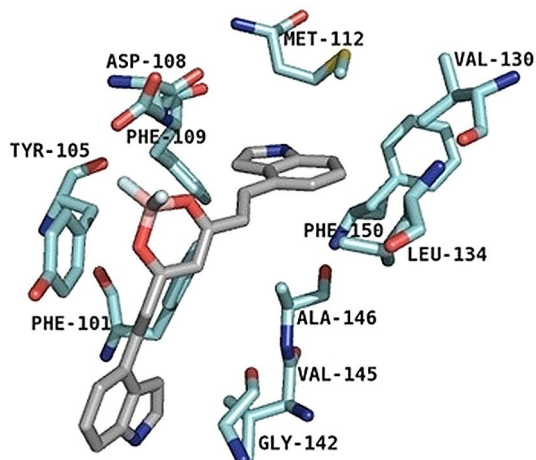


Figure 10. 3D Representation of 3-BF₂ in Bcl-2.

pounds proved to possess greater cancer-cell-specific cell growth inhibitory activity and lower toxicity to normal cells.

Studies aimed at understanding the mechanism of growth inhibition in CRC cells, and at improving aqueous solubility of this class of compounds as prerequisite for formulation and delivery are underway in our laboratories.

Experimental Section

Chemistry

General: The substituted benzaldehydes used in this study were all high-purity commercially available samples and were used without further purification. Regular solvents used for synthesis and isolation (MeCN, acetone, CH₂Cl₂, hexane, and EtOAc) were all of sufficient purity and were used as received. NMR spectra were recorded on a 500 MHz instrument using CDCl₃, [D₆]DMSO, or [D₆]acetone as solvent. ¹⁹F NMR were referenced relative to exter-

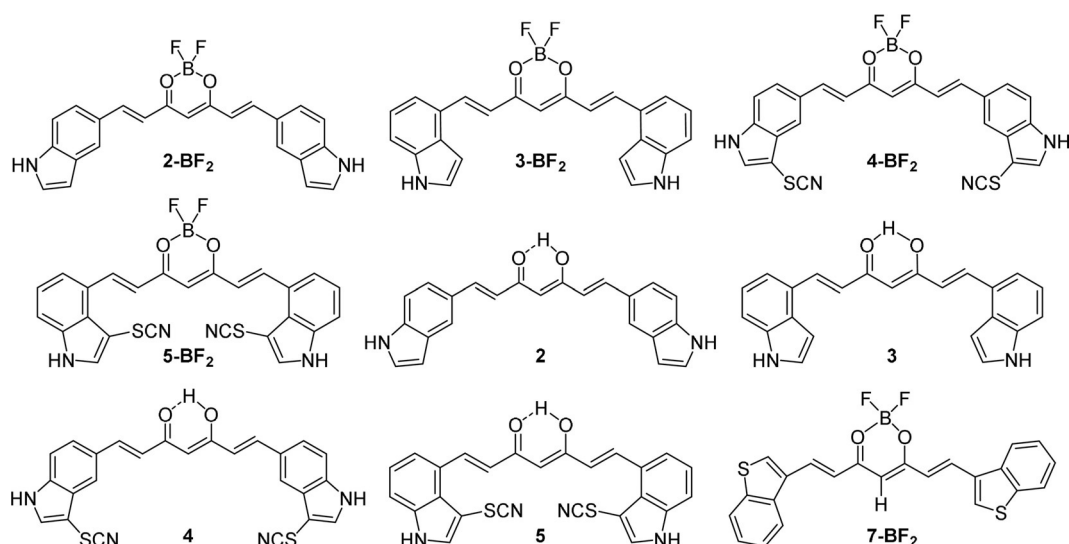


Figure 11. Compounds with high anti-proliferative and apoptotic activity based on NCI-60 assay data.

Compd	IC ₅₀ [nM] ^[a]			
	PBMCs	KMS11	MM1.S	RPMI-8226
3-BF ₂	50000	390	8340	2180
2	26900	1490	6680	11

[a] CUR analogue concentration at which 50% of cells remained viable after 72 h (CellTiter-Glo® assay).

Compd	KMS11	MM1.S	RPMI-8226
3-BF ₂	128	6.00	22.9
2	18.1	4.03	2445.5

[a] Tumor-specific lethality: (IC₅₀ PBMC)/(IC₅₀ tumor cell).

nal CFCl₃. HRMS analyses were performed on a Finnigan Quantum ultra-AM in electrospray mode using MeOH as solvent. Microwave reactions were performed in Biotage miniature 400 W lab microwave in 5 mL vials with magnetic stirring. FTIR spectra were recorded in ATR mode (as thin films formed via CH₂Cl₂ evaporation).

Melting points were measured in open capillaries and are not corrected.

General procedure for the synthesis of curcuminoid-BF₂ adducts: To a mixture of acetyl acetone-BF₂ complex (1 equiv) in EtOAc (minimal) under stirring and nitrogen atmosphere, the re-

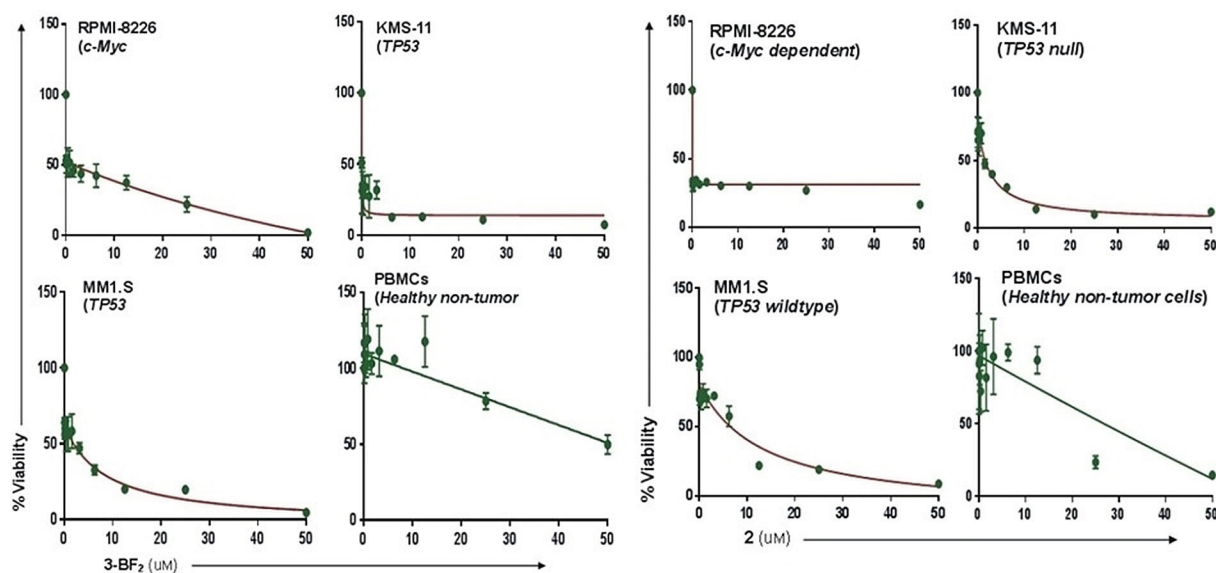


Figure 12. Cytotoxicity profiles for 3-BF₂ (left) and 2 (right) in MM cells relative to healthy cells. Cell proliferation and viability were determined in multiple myeloma (MM) cancer cell lines (RPMI-8226, KMS-11, and MM1.S) as well as in peripheral blood mononuclear cells (PBMCs) from healthy donors that were exposed to various concentrations of these CUR analogues for 72 h using the CellTiter-Glo® 2.0 assay. Error bars represent the mean ± SEM. All experiments were carried out in quadruplicates and conducted a minimum of two times.

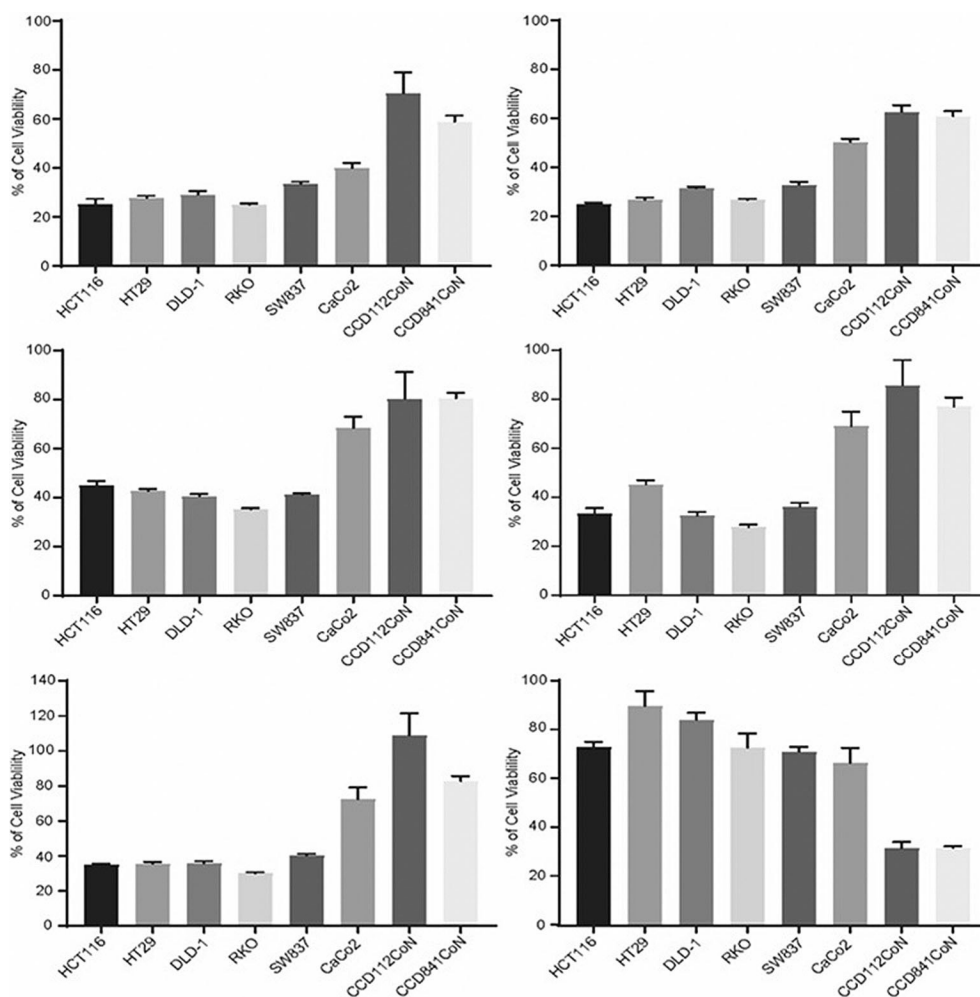


Figure 13. The CUR–BF₂ adducts showed significantly higher anticancer activity than the parent curcumin in CRC cells: 5-BF₂ (top left), 4-BF₂ (top right), 3-BF₂ (middle left), 7-BF₂ (middle right), 2-BF₂ (bottom left), curcumin (bottom right). CRC cells (HCT116, HT29, DLD-1, RKO, SW837, and CaCo2) and normal colon cells (CCD112CoN, CCD841CoN) were treated with DMSO or CUR compounds (10 μM) for 48 h. Error bars represent the mean ± SEM of two independent experiments performed in triplicate.

spective aldehyde (2.2 equiv) was added in one portion, followed by dropwise addition of *N*-butylamine (0.22 equiv) over a period of 20 min. The CUR–BF₂ adduct precipitated out of EtOAc upon overnight stirring at RT. The reaction mixture was subsequently cooled to 0 °C and the product was filtered, washed with cold (0 °C) EtOAc and dried under high vacuum, typically for 1 h.

Variations thereof—in cases where the product had precipitated but the yield was poor < 40%, the reaction mixture was returned to the flask with additional *N*-butylamine (0.22 equiv), and the reaction mixture was left to stir for an additional 48 h, whereupon additional product precipitated out of EtOAc. This was required for all of the indole-based curcuminoids, and for 8-BF₂. For 7-BF₂ the crude mixture was left at –20 °C for two days to harvest an additional crop.

General procedure for the decomplexation of CUR–BF₂: The curcuminoid–BF₂ complex (1 equiv) and sodium oxalate (2 equiv) were added to a 5 mL microwave vial equipped with a magnetic stir bar. Aqueous MeOH (5 mL, 8:2 MeOH/H₂O) was added and the vial was sealed with a crimp cap with septa. The sealed vial was irradiated at 100 W for 6 min at 140 °C with stirring set at 900 rpm. Decomplexation resulted in significant color change. The vial was cooled, the cap removed, and the reaction mixture was filtered,

washed with deionized water, and the product was dried for 15 min on the sinter and then under high vacuum.

Variations thereof: 7-BF₂ required four equivalents of sodium oxalate to fully decomplex in the microwave at 145 °C for 10 min.

Synthesis of the aryl pyrazole derivatives 10–15: These were synthesized by reacting the corresponding CUR compound with aryl pyrazoles in acetic acid using our previously described procedure.^[8]

Representative procedure: Curcuminoid 7 (60 mg, 0.155 mmol, 1 equiv) was added to a small Erlenmeyer flask along with 5 mL of glacial acetic acid, and phenyl hydrazine (67 mg, 0.62 mmol, 4 equiv) was then added. The reaction mixture was placed on a hotplate with stirring at 80 °C for 2 h. Following overnight mixing at room temperature, the reaction mixture was reheated at 80 °C, and H₂O was slowly added until the solution was almost turbid. The flask was then removed from the heat and left to cool in an ice bath. The product precipitated by cooling in an ice bath. It was washed with 3 × 5 mL portions of H₂O, and dried on high vacuum for 1 h to give 36 mg of a light-brown solid.

Variations: In the reaction with substituted phenyl hydrazines only 2 equivalents of the phenyl hydrazine was used. For compound **15**, the product had to be further purified by re-crystallization from Et₂O/hexane.

Indole-5-curcuminoid-BF₂ adduct (2-BF₂): Yield 65%, brown powder; *R_f*=0.11 (40% EtOAc in hexane). ¹H NMR ([D₆]acetone, 500 MHz): δ = 10.65 (brs, 2H), 8.18 (d, *J* = 16.0 Hz, 2H), 8.11 (s, 2H), 7.67 (dd, *J* = 8.5 Hz and 1.5 Hz, 2H), 7.56 (d, *J* = 8.5 Hz, 2H), 7.45 (unresolved dd, *J* = 3 Hz, 2H), 7.04 (d, *J* = 15.5 Hz, 2H), 6.62 (d, *J* = 3.0 Hz, 2H), 6.45 ppm (s, 1H); ¹³C NMR ([D₆]DMSO, 125 MHz): δ = 178.7, 148.7, 138.2, 128.2, 127.3, 125.6, 124.6, 122.0, 117.5, 112.5, 102.7, 101.2 ppm; ¹⁹F NMR ([D₆]acetone, 470 MHz): δ = -141.1 (s, ¹¹B-F), -141.2 ppm (s, ¹⁰B-F); IR: $\tilde{\nu}$ = 3418, 3005-2989, 1602, 1564, 1497, 1456, 1355, 1300, 1275, 1260, 1171, 1149, 1124, 1043 cm⁻¹.

Indole-5-curcuminoid-BF₂ adduct (2a-BF₂): (1,3-diketo tautomer in a mixture with **2-BF₂**): *R_f*=0.26 (40% EtOAc in hexane): ¹H NMR ([D₆]acetone, 500 MHz): δ = 8.16 (d, *J* = 16.0 Hz, 2H), 8.09 (unresolved, 2H), 7.61 (overlapping dd, 2H), 7.44 (unresolved, 2H), 7.0 (d, *J* = 16.0 Hz, 2H), 6.61 (unresolved, 2H), 6.43 ppm (s, 2H).

(1E,4E,6E)-5-Hydroxy-1,7-bis(indole-5)hepta-1,4,6-trien-3-one (2): Yield 94%, red-brown powder, mp: decomposes at 250 °C; *R_f*=0.38 (40% EtOAc in hexane); ¹H NMR ([D₆]DMSO, 500 MHz): δ = 11.35 (s, 2H), 7.90 (s, 2H), 7.74 (d, *J* = 16.0 Hz, 2H), 7.52 (d, *J* = 8.5 Hz, 2H), 7.44 (d, 8.0 Hz, s, 2H), 7.40 (brs, 2H), 6.82 (d, *J* = 16.0 Hz, 2H), 6.50 (brs, 2H), 6.11 ppm (s, 1H); ¹³C NMR ([D₆]DMSO, 125 MHz): δ = 183.7, 142.8, 137.7, 128.5, 127.2, 126.4, 122.8, 121.4, 121.1, 112.6, 102.9, 101.4 ppm; IR: $\tilde{\nu}$ = 3385, 2988, 2365, 1622, 1521, 1472, 1418, 1339, 1274, 1260, 1124 cm⁻¹; HRMS (ESI): *m/z* [M+H]⁺ calcd for C₂₃H₁₉O₂N₂: 355.1446, found: 355.1396.

Indole-4-curcuminoid-BF₂ adduct (3-BF₂): Yield 29%, black solid; *R_f*=0.16 (40% EtOAc in hexane). ¹H NMR ([D₆]acetone, 500 MHz): δ = 10.75 (brs, 2H), 8.45 (d, *J* = 16.0 Hz, 2H), 7.68 (d, 8.0 Hz, 2H), 7.64-7.62 (overlapping dd, and d, 4H), 7.27 (t, *J* = 8.0 Hz, 2H), 7.25 (d, *J* = 7.5 Hz, 2H), 6.95 (d, *J* = 3.5 Hz, 1H), 6.94 (brs, 1H), 6.57 ppm (s, 1H); ¹³C NMR ([D₆]DMSO, 125 MHz): δ = 179.7, 146.4, 137.1, 128.8, 127.4, 125.9, 124.0, 121.7, 121.1, 116.7, 102.4, 101.0 ppm; ¹⁹F NMR ([D₆]acetone, 470 MHz): δ = -140.6 (s, ¹¹B-F), -140.7 ppm (s, ¹⁰B-F); IR: $\tilde{\nu}$ = 3431, 3412, 2951-2930, 1613, 1597, 1541, 1483, 1433, 1389, 1354, 1296, 1153, 1119, 1044 cm⁻¹.

(1E,4E,6E)-5-Hydroxy-1,7-bis(indole-4)hepta-1,4,6-trien-3-one (3): Yield 77%, dark-brown solid, mp: 201-204 °C; *R_f*=0.42 (40% EtOAc in hexane); ¹H NMR ([D₄]MeOH, 500 MHz): δ = 8.08 (d, *J* = 15.5 Hz, 2H), 7.47 (d, *J* = 8.5 Hz, 2H), 7.40-7.39 (unresolved doublets, 4H), 7.17 (t, *J* = 7.5 Hz, 2H), 6.94 (d, *J* = 15.5 Hz, 2H), 6.85 (dd, *J* = 2.5 and 1 Hz, 2H), 6.13 ppm (s, 1H); ¹³C NMR ([D₄]MeOH, 125 MHz): δ = 183.7, 140.0, 136.9, 127.1, 126.5, 125.9, 123.3, 121.0, 119.9, 113.3, 101.1, 99.7 ppm; HRMS (ESI): *m/z* [M+H]⁺ calcd for C₂₃H₁₉O₂N₂: 355.1446, found: 355.1294; IR: $\tilde{\nu}$ = 3418, 3269-2872, 1620, 1557, 1416, 1344, 1277, 1201, 1141, 1111 cm⁻¹.

3-Thiocyanato-indole-5-curcuminoid-BF₂ adduct (4-BF₂): Yield 49%, reddish-orange solid; *R_f*=0.05 (40% EtOAc in hexane); ¹H NMR ([D₆]DMSO, 500 MHz): δ = 12.3 (s, 2H), 8.24 (d, *J* = 15.5 Hz, 2H), 8.25 (s, 2H), 8.11 (d, *J* = 2.5 Hz, 2H), 7.83 (dd, *J* = 8.5 Hz and 1.5 Hz, 2H), 7.63 (d, *J* = 8.5 Hz, 2H), 7.25 (d, *J* = 15.5 Hz, 2H), 6.74 ppm (s, 1H); ¹³C NMR ([D₆]DMSO, 125 MHz): δ = 179.8, 148.3, 138.6, 128.5, 128.1, 124.3, 121.7, 119.9, 114.2, 112.6, 102.0, 91.9 ppm; ¹⁹F NMR ([D₆]DMSO, 470 MHz): δ = -137.5 (s, ¹¹B-F), -137.6 ppm (s, ¹⁰B-F); IR: $\tilde{\nu}$ = 3417, 2916, 2848, 2152, 1739, 1612, 1552, 1541, 1500, 1382, 1300, 1058 cm⁻¹.

(1E,4E,6E)-5-Hydroxy-1,7-bis(3-thiocyanatoindole-5)hepta-1,4,6-trien-3-one (4): Yield 73%, red solid, mp: decomposes at 250 °C; *R_f*=0.08 (40% EtOAc in hexane). ¹H NMR ([D₆]DMSO, 500 MHz): δ = 16.3 (brs, 1H), 12.21 (d, *J* = 2 Hz, 2H), 8.06 (d, *J* = 2.5 Hz, 2H), 8.03 (s, 2H), 7.86 (d, *J* = 16.0 Hz, 2H), 7.70 (d, *J* = 9.0 Hz, 2H), 7.58 (d, *J* = 8.5 Hz, 2H), 6.96 (d, *J* = 16.0 Hz, 2H), 6.30 ppm (s, 1H); ¹³C NMR ([D₆]DMSO, 125 MHz): δ = 183.7, 141.8, 138.0, 135.0, 128.6, 128.4, 123.3, 123.1, 119.6, 114.0, 112.7, 101.6, 91.2 ppm; HRMS (ESI): *m/z* [M+H]⁺ calcd for C₂₅H₁₆O₂N₄S₂: 469.56574, found: 469.47375; IR: $\tilde{\nu}$ = 3300, 2924, 2152, 1705, 1622, 1604, 1273, 1138, 1124, 958 cm⁻¹.

3-Thiocyanato-indole-4-curcuminoid-BF₂ adduct (5-BF₂): Yield 62%, dark-brown powder; *R_f*=0.09 (40% EtOAc in hexane). ¹H NMR ([D₆]acetone, 500 MHz): δ = 9.34 (d, *J* = 15.0 Hz, 2H), 8.14 (d, 2.0 Hz, 2H), 7.90 (d, *J* = 7.0 Hz, 2H), 7.77 (d, *J* = 7.0 Hz, 2H), 7.42* (t, *J* = 8.0 Hz, 2H), 7.27* (d, *J* = 16.5 Hz, 2H), 6.71 cm⁻¹ (s, 1H); [NH signal is observed in [D₆]DMSO at δ = 12.39 (s, 2H) in which signals marked with * are overlapping]; ¹³C NMR ([D₆]DMSO, 125 MHz): δ = 180.0, 142.8, 138.0, 137.5, 126.9, 125.9, 123.7, 122.5, 121.7, 117.3, 113.1, 103.1, 90.4 ppm; ¹⁹F NMR ([D₆]DMSO, 470 MHz): δ = -137.5 (s, ¹¹B-F), -137.6 ppm (s, ¹⁰B-F); IR: $\tilde{\nu}$ = 3395, 3335, 2154, 2156, 1616, 1601, 1555, 1541, 1508, 1493, 1410, 1275, 1161, 1128, 1062 cm⁻¹.

(1E,4E,6E)-5-Hydroxy-1,7-bis(3-thiocyanatoindole-4)hepta-1,4,6-trien-3-one (5): Yield 82%, red powder, decomposes at 250 °C; *R_f*=0.10 (40% EtOAc in hexane). ¹H NMR ([D₆]DMSO, 500 MHz): δ = 12.27 (s, 2H), 9.00 (d, *J* = 15.5 Hz, 2H), 8.12 (d, *J* = 2 Hz, 2H), 7.74 (d, *J* = 8.0 Hz, 2H), 7.61 (d, *J* = 8.0 Hz, 2H), 7.33 (t, *J* = 7.5 Hz, 2H), 7.04 (d, *J* = 16.0 Hz, 2H), 6.24 ppm (s, 1H); ¹³C NMR ([D₆]DMSO, 125 MHz): δ = 183.6, 137.9, 136.9, 136.7, 127.8, 125.6, 125.3, 123.7, 120.3, 115.4, 113.3, 102.6, 90.0 ppm; IR: $\tilde{\nu}$ = 3313, 2155, 1624, 1602, 1396, 1275, 1119 cm⁻¹; HRMS (ESI): *m/z* [M+H]⁺ calcd for C₂₅H₁₇O₂N₄S₂: 469.07929, found: 469.3449

N-methylindole-3-curcuminoid-BF₂ adduct (6-BF₂): Yield 60%, dark-green solid; *R_f*=0.32 (40% EtOAc in hexane). ¹H NMR ([D₆]acetone, 500 MHz): δ = 8.20 (d, *J* = 15.5 Hz, 2H), 8.10 (d, *J* = 7.5 Hz, 2H), 8.03 (s, 2H), 7.58 (d, *J* = 8.5 Hz, 2H), 7.38 (dt, *J* = 7 Hz and 1 Hz, 2H), 7.33 (dt, *J* = 7 Hz and 1 Hz, 2H), 6.90 (d, *J* = 15.5 Hz, 2H), 6.39 (s, 1H), 4.0 cm⁻¹ (s, 6H); ¹³C NMR ([D₆]acetone, 125 MHz): δ = 178.1, 139.3, 138.9, 138.0, 126.0, 123.4, 122.0, 120.7, 115.0, 113.2, 110.9, 100.1, 32.8 ppm; ¹⁹F NMR ([D₆]acetone, 470 MHz): δ = -142.0 (s, ¹¹B-F), -141.9 ppm (s, ¹⁰B-F); IR: $\tilde{\nu}$ = 1599, 1557, 1501, 1456, 1445, 1422, 1389, 1371, 1340, 1371, 1287, 1251, 1153, 1124, 1072 cm⁻¹.

(1E,4E,6E)-5-Hydroxy-1,7-bis(N-methylindole-3)hepta-1,4,6-trien-3-one (6): Yield 98%, bright-red powder, mp: 195-198 °C; *R_f*=0.54. ¹H NMR ([D₆]acetone, 500 MHz): δ = 8.04 (d, *J* = 8 Hz, 2H), 7.91 (d, *J* = 16.0 Hz, 2H), 7.78 (s, 2H), 7.52 (d, *J* = 8.5 Hz, 2H), 7.33 (t, *J* = 7 Hz, 2H), 7.26 (t, *J* = 8.5 Hz, 2H), 6.77 (d, *J* = 15.5 Hz, 2H), 6.04 (s, 1H), 3.92 ppm (s, 6H); ¹³C NMR ([D₆]acetone, 500 MHz): δ = 183.8, 138.5, 134.4, 133.5, 126.1, 122.7, 121.1, 120.3, 118.9, 112.5, 110.4, 100.1, 32.5 ppm; HRMS (ESI): *m/z* [M+H]⁺ calcd for C₂₅H₂₃O₂N₂: 383.17595, found: 383.16476; IR: $\tilde{\nu}$ = 3100 to 2824, 1746, 1715, 1607, 1556, 1519, 1494, 1454, 1421, 1373, 1330, 1255, 1157, 1126, 1070 cm⁻¹.

N-methylindole-3-curcuminoid-BF₂ adduct (1,3-diketo tautomer; 6a-BF₂): Yield 22%, deep-purple solid; *R_f*=0.44 (40% EtOAc in hexane); ¹H NMR ([D₆]DMSO, 500 MHz): δ = 8.31 (d, *J* = 15.5 Hz, 2H), 8.26 (s, 2H), 8.12 (d, *J* = 7 Hz, 2H), 7.62 (d, *J* = 8 Hz, 2H), 7.39 (t, *J* = 7 Hz, 2H), 7.33 (t, *J* = 7 Hz, 2H), 6.85 (d, *J* = 15.5 Hz, 2H), 6.40 (s, 2H), 3.89 ppm (s, 6H); ¹³C NMR ([D₆]DMSO, 125 MHz): δ = 186.3, 181.0, 143.8, 141.4, 139.1, 125.7, 124.2, 123.1, 121.3, 113.0, 112.8,

112.0, 100.4, 34.0, 23.9 ppm; ^{19}F NMR ($[\text{D}_6]\text{DMSO}$, 470 MHz): $\delta = -137.6$ (s, $^{11}\text{B-F}$), -137.5 ppm (s, $^{10}\text{B-F}$); IR: $\tilde{\nu} = 3055, 2988, 1620, 1558, 1516, 1375, 1294, 1263, 1169, 1063$ ppm.

(1E,6E)-1,7-bis(N-methylindole-3)hepta-1,6-dien-3,5-dione (6a): Yield 64%, light-red powder, mp: 126–128 °C; $R_f = 0.72$ (40% EtOAc in hexane). ^1H NMR (CDCl_3 , 500 MHz): $\delta = 7.93$ (d, $J = 8$ Hz, 2H), 7.85 (d, $J = 15.5$ Hz, 2H), 6.49 (d, $J = 15.5$ Hz, 2H), 5.41 (s, 2H), 3.82 ppm (s, 6H); ^{13}C NMR (CDCl_3 , 125 MHz): $\delta = 194.7, 180.5, 138.2, 134.0, 133.2, 126.0, 123.0, 121.3, 120.5, 117.7, 112.8, 110.1, 99.9, 33.2, 26.3$ ppm; HRMS (ESI): m/z $[M+H]^+$ calcd for $\text{C}_{25}\text{H}_{12}\text{O}_2\text{N}_2$: 383.17595, found: 383.16467; IR: $\tilde{\nu} = 3098$ to 2914, 1716, 1626, 1534, 1422, 1375, 1263, 1159, 1132, 1072 cm^{-1} .

Benzothiophene-3-curcuminoid-BF₂ adduct (7-BF₂): Yield: 70%, bright-orange solid, mp: > 240 °C; $R_f = 0.81$ (40% EtOAc in hexane). ^1H NMR ($[\text{D}_6]\text{DMSO}$, 500 MHz): $\delta = 8.75$ (s, 2H), 8.33 (d, $J = 20$ Hz, 2H), 8.34 (s, 2H), 8.14 (d, $J = 8.0$ Hz, 2H), 7.58 (t, $J = 7.5$ Hz, 2H), 7.52 (t, $J = 7.5$ Hz, 2H), 7.30 (d, $J = 16.0$ Hz, 2H), 6.97 ppm (s, 1H); ^{13}C NMR ($[\text{D}_6]\text{DMSO}$, 125 MHz): $\delta = 180.2, 140.5, 138.5, 136.9, 135.8, 132.1, 126.1, 124.0, 123.0, 121.7, 110.0, 102.3$ ppm; ^{19}F NMR ($[\text{D}_6]\text{DMSO}$, 470 MHz): $\delta = -137.4$ (s, $^{11}\text{B-F}$), -137.3 ppm (s, $^{10}\text{B-F}$).

(1E,4E,6E)-5-Hydroxy-1,7-bis(benzo[b]thiophen-3-yl)hepta-1,4,6-trien-3-one (7): Yield: 85%, orange solid, mp: 159–160 °C; $R_f = 0.74$ (40% EtOAc in hexane); ^1H NMR ($[\text{D}_6]\text{DMSO}$, 500 MHz): $\delta = 8.43$ (s, 2H), 8.22 (d, $J = 7.5$ Hz, 2H), 8.09 (d, $J = 7.5$ Hz, 2H), 8.79 (d, $J = 16.5$ Hz, 2H), 7.53 (t, $J = 7.5$ Hz, 2H), 7.48 (t, $J = 7.5$ Hz, 2H), 7.05 (d, $J = 16.5$ Hz, 2H), 6.44 ppm (s, 1H); ^{13}C NMR ($[\text{D}_6]\text{DMSO}$, 125 MHz): $\delta = 183.7, 140.4, 137.3, 132.4, 132.1, 130.6, 125.7, 125.2, 123.8, 122.7, 102.0$ ppm; HRMS (ESI): m/z $[M+H]^+$ calcd for $\text{C}_{23}\text{H}_{17}\text{O}_2\text{S}_2$: 389.06700, found: 389.06055; IR: $\tilde{\nu} = 3093$ to 2852, 1614, 1489, 1421, 1269, 1134, 958 cm^{-1} .

Benzothiophene-2-curcuminoid-BF₂ adduct (8-BF₂): Yield 28%, black solid; $R_f = 0.85$ (40% EtOAc in hexane). ^1H NMR ($[\text{D}_6]\text{DMSO}$, 500 MHz): $\delta = 8.38$ (d, $J = 15.5$ Hz, 2H), 8.11 (s, 2H), 8.06 (d, $J = 8.0$ Hz, 2H), 7.97 (d, $J = 7.5$ Hz, 2H), 7.51 (dt, $J = 7.5$ and 1.5 Hz, 2H), 7.46 (dt, $J = 8.0$ and 1.5 Hz, 2H), 6.89 (d, $J = 15$ Hz, 2H), 6.83 ppm (s, 1H); ^{13}C NMR ($[\text{D}_6]\text{DMSO}$, 125 MHz): $\delta = 179.5, 141.4, 140.5, 140.0, 139.8, 133.8, 128.1, 125.9, 123.4, 122.5, 110.0, 103.5$ ppm; ^{19}F NMR ($[\text{D}_6]\text{DMSO}$, 470 MHz): $\delta = -137.2$ (s, $^{11}\text{B-F}$), -137.3 ppm (s, $^{10}\text{B-F}$); IR: $\tilde{\nu} = 3057$ to 2851, 1599, 1533, 1485, 1385, 1283, 1136, 1051 cm^{-1} .

(1E,4E,6E)-5-Hydroxy-1,7-bis(benzo[b]thiophen-2-yl)hepta-1,4,6-trien-3-one (8): Yield 93%, orange solid; $R_f = 0.92$ (40% EtOAc in hexane). ^1H NMR ($[\text{D}_6]\text{DMSO}$, 500 MHz): $\delta = 16.0$ (brs, 1H), 8.00 (d, $J = 7.5$ Hz, 2H), 7.97 (d, $J = 16$ Hz, 2H), 7.90 (d, $J = 7.0$ Hz, 2H), 7.87 (s, 2H), 7.45 (dt, $J = 7.5$ and 2 Hz, 2H), 7.41 (dt, $J = 7.5$ and 2.0 Hz, 2H), 6.65 (d, $J = 16$ Hz, 2H), 6.36 ppm (s, 1H); HRMS (ESI): m/z $[M+H]^+$ calcd for $\text{C}_{23}\text{H}_{17}\text{O}_2\text{S}_2$: 389.06700, found: 389.05377.

Benzofuran-2-curcuminoid-BF₂ adduct (9-BF₂): Yield: 70%, dark-red solid, mp: > 240 °C; $R_f = 0.84$ (40% EtOAc in hexane); ^1H NMR (CDCl_3 , 500 MHz): $\delta = 7.91$ (d, $J = 15.0$ Hz, 2H), 7.65 (d, $J = 7.5$ Hz, 2H), 7.53 (dd, $J = 8.5$ Hz, 2H), 7.45 (dt, $J = 7.0$ Hz and 1.0 Hz, 2H), 7.23 (dt, $J = 7.0$ Hz and 1.0 Hz, 2H), 7.14 (s, 2H), 6.88 (d, $J = 15.5$ Hz, 2H), 6.16 ppm (s, 1H); ^{13}C NMR (CDCl_3 , 125 MHz): $\delta = 179.3, 156.4, 152.3, 132.8, 128.5, 127.9, 123.9, 122.5, 120.9, 115.5, 111.6, 103.5$ ppm; ^{19}F NMR (CDCl_3 , 470 MHz): $\delta = -140.15$ (s, $^{11}\text{B-F}$), -140.1 ppm (s, $^{10}\text{B-F}$); IR: $\tilde{\nu} = 2918, 1614, 1557, 1508, 1396, 1348, 1288, 1155, 1124, 1057, 947$ cm^{-1} .

(1E,4E,6E)-5-Hydroxy-1,7-bis(benzo[b]furan-2-yl)hepta-1,4,6-trien-3-one (9): Yield: 88% yellow-orange solid, mp: 178–180 °C; $R_f = 0.92$ (40% EtOAc in hexane); ^1H NMR ($[\text{D}_6]\text{acetone}$, 500 MHz):

$\delta = 7.73$ (dd, $J = 7.5$ and 1.5 Hz, 2H), 7.67 (d, $J = 15.0$ Hz, 2H), 7.59 (d, $J = 7.5$ Hz, 2H), 7.44 (dd, $J = 7.5$ and 1.5 Hz, 2H), 7.31 (dt, $J = 7.5$ and 1.7 Hz, 2H), 7.31 (s, 2H), 6.91 (d, $J = 15.0$ Hz, 2H), 6.31 ppm (s, 1H); ^{13}C NMR (CDCl_3 , 125 MHz): $\delta = 182.5, 155.7, 153.1, 128.6, 127.2, 126.5, 124.6, 123.4, 121.7, 111.4, 111.3, 103.3$ ppm; HRMS (ESI): m/z $[M+H]^+$ calcd for $\text{C}_{23}\text{H}_{17}\text{O}_4$: 357.11268, found: 357.10632; IR: $\tilde{\nu} = 3080, 2953, 1608, 1557, 1516, 1348, 1286, 1256, 1200$ cm^{-1} .

3,5-bis((E)-(benzo[b]thiophen-3-yl)vinyl)-1-phenyl-1H-pyrazole (10): Yield: 50%, light-brown/orange solid, mp: 141–143 °C; $R_f = 0.87$ (40% EtOAc in hexane); ^1H NMR (CDCl_3 , 500 MHz): $\delta = 8.10$ (d, $J = 8.0$ Hz, 1H), 7.94 (d, $J = 8.0$ Hz, 1H), 7.90 (d, $J = 8.0$ Hz, 1H), 7.89 (d, $J = 8.0$ Hz, 1H), 7.39–7.47 (m, unresolved, 6H), 7.62–7.52 (m, unresolved, 7H), 7.31 (d, $J = 16.0$ Hz, 1H), 7.01 (s, 1H), 6.98 ppm (d, $J = 16.5$ Hz, 1H); ^{13}C NMR (CDCl_3 , 125 MHz): $\delta = 151.2, 142.5, 140.5, 139.3, 127.7, 137.4, 133.8, 133.2, 129.4, 128.2, 125.5, 124.8, 124.6, 124.6, 124.5, 124.4, 123.4, 123.1, 123.0, 122.6, 122.1, 121.8, 121.5, 116.7, 101.0$ ppm; HRMS (ESI): m/z $[M+H]^+$ calcd for $\text{C}_{29}\text{H}_{20}\text{N}_2\text{S}_2$: 461.11462, found: 461.10458; IR: $\tilde{\nu} = 3028, 3010, 1694, 1645, 1633, 1603, 1494, 1440, 1404, 1373, 1249, 1153, 1028$ cm^{-1} .

3,5-bis((E)-(benzo[b]thiophen-3-yl)vinyl)-1-(3-(trifluoromethyl)phenyl)-1H-pyrazole (11): Yield 63.0%, light-brown solid, mp: 95–96 °C; $R_f = 0.91$ (40% EtOAc in hexane); ^1H NMR (CDCl_3 , 500 MHz): $\delta = 8.11$ (d, $J = 8.5$ Hz, 1H), 7.96 (d, $J = 8.5$ Hz, 1H), 7.95 (s, 1H), 7.91 (d, $J = 8.0$ Hz, 2H), 7.79 (d, $J = 7.5$ Hz, 1H), 7.78 (d, $J = 7.5$ Hz, 1H), 7.72 (d, $J = 7.5$ Hz, 1H), 7.67 (d, $J = 7.5$ Hz, 1H), 7.64 (s, 1H), 7.56 (d, $J = 15.5$ Hz, 1H), 7.54 (s, 1H), 7.50–7.40 (m, unresolved, 5H), 7.30 (d, $J = 16.5$ Hz, 1H), 7.03 (s, 1H), 6.97 ppm (d, $J = 16.5$ Hz, 1H); ^{13}C NMR (CDCl_3 , 125 MHz): $\delta = 151.9, 142.7, 140.6, 140.6, 139.9, 137.6, 137.3, 133.7, 133.0, 132.0$ (q, $^1J_{\text{CF}} = 250$ Hz), 130.0, 128.3, 125.5, 124.9, 124.7, 124.7, 124.6, 124.4, 124.0, 123.5, 123.1, 123.0, 122.9, 122.2 (q, $J_{\text{CF}} = 3.5$ Hz), 122.1, 121.8, 121.2, 116.0, 101.7 ppm; ^{19}F NMR (CDCl_3 , 470 MHz): $\delta = -62.60$ (s, CF_3); HRMS (ESI): m/z $[M+H]^+$ calcd for $\text{C}_{30}\text{H}_{19}\text{N}_2\text{F}_3$: 529.102001, found: 529.10034; IR: $\tilde{\nu} = 3067, 1699, 1614, 1597, 1497, 1456, 1423, 1377, 1360, 1325, 1277, 1263, 1168, 1126, 1093, 1067, 1022$ cm^{-1} .

3,5-bis((E)-(benzo[b]thiophen-3-yl)vinyl)-1-(3,5-difluorophenyl)-1H-pyrazole (12): Yield: 50%, yellow solid, mp: 178–179 °C; $R_f = 0.85$ (40% EtOAc in hexane); ^1H NMR (CDCl_3 , 500 MHz): $\delta = 8.09$ (d, $J = 8.0$ Hz, 1H), 7.97 (d, $J = 8.0$ Hz, 1H), 7.91 (d, $J = 8.0$ Hz, 1H), 7.90 (d, $J = 7.5$ Hz, 1H), 7.62 (s, 1H), 7.58 (s, 1H), 7.53 (d, $J = 16.0$ Hz, 1H), 7.39–7.40 (unresolved region, 5H), 7.27–7.19 (unresolved region, 2H), 7.00 (d, $J = 17.0$ Hz, 2H), 6.98 (s, 1H), 6.89 ppm (tt, $J = 5.5$ Hz and 2.5 Hz, 1H); ^{13}C NMR (CDCl_3 , 125 MHz): $\delta = 163.1$ (d, $^1J_{\text{CF}} = 249.0$ Hz), 163.0 (d, $^1J_{\text{CF}} = 249.0$ Hz), 152.0, 142.7, 141.4 (t, $^3J_{\text{CF}} = 12.3$ Hz), 140.6, 140.5, 137.6, 137.3, 133.6, 133.0, 125.5, 124.9, 124.7, 124.7, 124.5, 123.9, 123.7, 123.1, 123.0, 122.9, 122.1, 121.7, 121.1, 116.0, 108.4, 103.3 (t, $^2J_{\text{CF}} = 25.7$ Hz), 102.3 ppm; ^{19}F NMR (CDCl_3 , 470 MHz): $\delta = -107.37$ (m, 2F); HRMS (ESI): m/z $[M+H]^+$ calcd for $\text{C}_{29}\text{H}_{19}\text{N}_2\text{S}_2\text{F}_2$: 497.09577, found: 497.08199; IR: $\tilde{\nu} = 3080, 1620, 1597, 1539, 1481, 1462, 1425, 1304, 1263, 1223, 1119$ cm^{-1} .

3,5-bis((E)-(benzofuran-2-yl)vinyl)-1-phenyl-1H-pyrazole (13): Yield: 67%, yellow solid, mp: 149–151 °C; $R_f = 0.95$ (40% EtOAc in hexane). ^1H NMR (CDCl_3 , 500 MHz): $\delta = 7.57$ –7.47 (unresolved region, 8H), 7.54 (d, $J = 8.0$ Hz, 2H), 7.35 (d, $J = 17.5$ Hz, 1H), 7.30–7.26 (complex region, 2H), 7.21 (t, $J = 8.0$ Hz, 2H), 7.18 (d, $J = 16.5$ Hz, 1H), 7.09 (d, $J = 15.5$ Hz, 1H), 7.00 (d, $J = 16.0$ Hz, 1H), 6.87 (s, 1H), 6.73 (s, 1H), 6.71 ppm (s, 1H); ^{13}C NMR (CDCl_3 , 125 MHz): $\delta = 155.0, 155.0, 154.8, 153.9, 150.4, 141.9, 139.2, 129.4, 129.1, 128.8, 128.3, 125.6, 125.2, 124.7, 123.1, 122.9, 121.5, 121.1, 120.9, 119.9, 118.6, 116.3, 111.0, 106.9, 105.5, 102.2$ ppm; HRMS (ESI): m/z $[M+H]^+$ calcd for $\text{C}_{29}\text{H}_{21}\text{N}_2\text{O}_2$: 429.16030, found: 429.15786; IR

(CH₂Cl₂): 3055, 2924, 1713, 1597, 1497, 1451, 1366, 1288, 1250, 1188, 1126, 1011 cm⁻¹.

3,5-bis((E)-(benzofuran-2-yl)vinyl)-1-(3,5-difluorophenyl)-1H-pyrazole (14): Yield: 54%, yellow solid, mp: 158–160 °C; *R*_f=0.91 (40% EtOAc in hexane); ¹H NMR (CDCl₃, 500 MHz): δ = 7.57–7.54 (overlapping pair of doubles, triplet appearance, 2H), 7.50–7.46 (overlapping pair of doubles, triplet appearance, 2H), 7.34–7.15 (unresolved region, 8H), 7.14 (d, *J* = 16.0 Hz, 1H), 7.06 (d, *J* = 16 Hz, 1H), 6.93 (tt, *J* = 9.0 Hz and 2.0 Hz, 1H), 6.86 (s, 1H), 6.78 (s, 1H), 6.74 ppm (s, 1H); ¹³C NMR (CDCl₃, 125 MHz): δ = 163.1 (d, ¹*J*_{CF} = 249.0 Hz), 163.0 (d, ¹*J*_{CF} = 249.0 Hz) 155.2, 155.0, 154.5, 153.5, 151.1, 142.1, 141.2 (t, ³*J*_{CF} = 12.4 Hz), 129.0, 128.8, 125.5, 124.9, 123.2, 123.0, 121.2, 121.1, 121.0, 120.8, 119.2, 115.4, 111.1, 111.0, 108.6, 107.5, 105.9, 103.5 (t, ²*J*_{CF} = 25.7 Hz), 103.2 ppm; ¹⁹F NMR (CDCl₃, 470 MHz): δ = -107.4 (m, 2F); HRMS (ESI): *m/z* [*M* + H]⁺ calcd for C₂₉H₁₉N₂O₂F₂: 465.14146, found: 465.13156; IR: $\tilde{\nu}$ = 3086 to 2926, 1620, 1600, 1562, 1526, 1481, 1450, 1381, 1348, 1329, 1285, 1254, 1225, 1196, 1118 cm⁻¹.

3,5-bis((E)-(benzofuran-2-yl)vinyl)-1-(3-(trifluoromethoxy)phenyl)-1H-pyrazole (15): Yield: 22%, light brown solid, mp: 128–129 °C; *R*_f = 0.96 (40% EtOAc in hexane); ¹H NMR (CDCl₃, 500 MHz): δ = 7.63 (overlapping pair of doubles, 2H), 7.57 (d, *J* = 7.5 Hz, 1H), 7.56 (d, *J* = 8.0 Hz, 1H), 7.50 (d, 8 Hz, 1H), 7.46–7.42 (unresolved, 3H), 7.35–7.22 (complex region, 5H), 7.18 (d, *J* = 16.0 Hz, 1H), 7.07 (d, *J* = 16.0 Hz, 1H), 7.03 (d, *J* = 16.0 Hz, 1H), 6.89 (s, 1H), 6.77 (s, 1H), 6.73 ppm (s, 1H); ¹³C NMR (CDCl₃, 125 MHz): δ = 150.3, 150.2, 149.9, 148.9, 146.1, 143.9, 137.3, 133.0, 124.3, 124.0, 122.0, 120.6, 120.0, 118.4, 118.2, 117.1, 116.6, 116.4, 116.1, 115.5, 114.0, 111.0, 106.3, 106.3, 102.5, 101.0, 97.8 ppm; ¹⁹F NMR (CDCl₃, 470 MHz): δ = 57.83 ppm (s, OCF₃); HRMS (ESI): *m/z* [*M* + H]⁺ calcd for C₃₀H₂₀N₂O₃F₃: 513.14260, found: 513.13940; IR: $\tilde{\nu}$ = 3116 to 2926, 1717, 1668, 1609, 1564, 1510, 1452, 1371, 1384, 1254, 1205, 1161, 1033, 1015 cm⁻¹.

Computational studies

B3LYP/6-31G*^[19] geometry optimizations were performed with the Gaussian 09 suite of programs.^[20] Molecular docking calculations were carried out with the program AutoDock Vina (version 1.1.2)^[21] for modeling the binding modes and gauging the interaction energies of the studied compounds as ligands for HER2, proteasome, VEGFR2, BRAF, and Bcl-2 proteins. The three-dimensional coordinates of the proteins were obtained from the RCSB Protein Data Bank (PDB IDs: 3PP0^[22] (HER2), 3SDK^[23] (20S proteasome), 4AG8^[16] (VEGFR2), 4XV2^[17] (BRAF), and 4LVT^[18] (Bcl-2)). Chain A of HER2, VEGFR2, BRAF and Bcl-2, and chains K (β5 subunit) and L (β6 subunit) of 20S proteasome were selected as target templates for the docking calculations. Co-crystallized ligands and crystallographic water molecules were removed. Addition of hydrogens, merger of nonpolar hydrogens to the atom to which they were attached, and assignment of partial charges were computed with AutoDockTools. Docking areas were constrained to a 30 × 30 × 30 Å box centered at the active site, which provided suitable space for rotational and translational movement of the ligands.

Bioassays

NCI-60 assay: Samples were submitted to the National Cancer Institute (NCI of NIH) Developmental Therapeutics anticancer screening program (DTP) for human tumor cell line assay by NCI-60 screening against leukemia, lung, colon, and CNS cancers, as well as melanoma, ovarian, renal, prostate, and breast cancers. Com-

pounds are initially tested at a single dose of 10⁻⁵ molar. Data are reported as mean graph of percent growth (GP). Growth inhibition is shown by values between 0 and 100 and lethality by values less than zero. Compounds that meet selection criteria based on one-dose assay are then tested against 60 cell panel at five concentrations. More details on operating procedures and sample preparation are reported here: https://dtp.cancer.gov/discovery_development/nci-60/methodology.htm (last accessed July 23, 2018).

Cell viability assay to determine EC₅₀: Multiple myeloma cell lines, MM1.S, KMS-11, and RPMI-8226 were used as well as healthy donor peripheral blood mononuclear cells from healthy donors, as previously described.^[24] Cells (2 × 10³ cells per well) were incubated with the compounds (concentration range 0–30 000 nM) in a 384-well plate for 72 h in a CO₂ incubator (5% CO₂, 37 °C). Cell lines and PBMCs (as noncancer control) were seeded in quadruplicate (technical replicates). CellTiter-Glo[®] 2.0 reagent equal to the volume of cell culture medium present in each well was added and the plate was left to incubate at room temperature for 10 min to stabilize the luminescent signal. Luminescent signal/intensity from the 384-well plate was read on a plate reader.

Cell culture: Multiple myeloma cell lines were cultured in RPMI-1640 medium containing 10% FBS and penicillin (100 gmL⁻¹) and streptomycin (100 gmL⁻¹). Culture medium was replaced every 3 d. Cell viability was always maintained at >90% and was measured by trypan blue exclusion assay using a ViCell-XR viability counter.

Apoptosis assay: Apoptosis was measured using the Annexin-V binding assay kit from BD Biosciences (San Diego, CA, USA) according to the manufacturer's instructions, and as previously described.^[25] Briefly, at the end of the treatment, cells were washed with PBS and 1 × 10⁶ cells were re-suspended in 100 μL binding buffer. Fluorescein isothiocyanate (FITC)-labelled Annexin-V (5 μL) and PI (10 μL) were added to each sample and incubated in the dark for 15 min at room temperature. The cells were subsequently analyzed by flow cytometry using BD Accuri, the C6 flow cytometer and its software. Data from 10 000 events per sample were collected and analyzed.

Cell viability assay for colorectal cells: Colorectal cancer and normal colon cell lines were obtained from the American Type Culture Collection (ATCC, Manassas, VA, USA). Cells were maintained in DMEM (Life Technologies, Carlsbad, CA, USA) supplemented with 10% fetal bovine serum (Life Technologies), 1% non-essential amino acids (Life Technologies), 1% penicillin–streptomycin (Life Technologies), and 1% glutamine (Life Technologies) at 37 °C and 5% CO₂. Cells were seeded in 96-well plates with approximately 5.0 × 10³ cells per well and incubated in RPMI-1640 medium (supplemented with 10% fetal bovine serum and 1% glutamine) for 24 h. Cells were then treated with RPMI-1640 medium containing CUR compounds (10 μM) or vehicle (DMSO) for 48 h and the number of viable cells were determined using CellTiter-Fluor[™] cell viability assay kit (Promega, Madison, WI, USA). The fluorescence (excitation 400 nm, emission 505 nm) was detected using infinite M200 Pro microplate reader (TECAN).

Acknowledgements

K.K.L. thanks the University of North Florida (UNF) for the outstanding faculty scholarship and presidential professorship awards, a faculty scholarship, and UNF Foundation Board grants. G.L.B. acknowledges funding from CONICET and Secyt-UNC. We also acknowledge the Developmental Therapeutics Program

(DTP) of the US National Cancer Institute for *in vitro* anticancer screening. Work at the Mayo Clinic was supported by a grant from the Daniel Foundation of Alabama (A.C.-K.). It also received support from the University of Iowa and Mayo Clinic Lymphoma SPOR, Developmental Research Program (P50 CA097274) (A.P.). We also acknowledge support from the Mayo Clinic Cancer Center (CA015083) (A.C.-K.).

Conflict of interest

The authors declare no conflict of interest.

Keywords: antitumor agents · apoptosis · binding affinity · curcuminoids · multiple myeloma

- [1] S. C. Gupta, S. Prasad, J. H. Kim, S. Patchva, L. J. Webb, I. K. Priyadarini, B. B. Aggarwal, *Nat. Prod. Rep.* **2011**, *28*, 1937–1955.
- [2] A. Minassi, G. Sánchez-Duffhues, J. A. Collado, E. Muñoz, G. Appendino, *J. Nat. Prod.* **2013**, *76*, 1105–1112.
- [3] K. Bairwa, J. Grover, M. Kania, S. M. Jachak, *RSC Adv.* **2014**, *4*, 13946–13978.
- [4] V. P. Dandawate, P. S. Padhye, A. Ahmad, A. F. Sarkar, *Curr. Pharm. Des.* **2013**, *19*, 2047–2069.
- [5] a) G. R. Pillai, A. S. Srivastava, T. I. Hassanein, D. P. Chauhan, E. Carrier, *Cancer Lett.* **2004**, *208*, 163–170; b) A. L. Lopresti, S. D. Hood, P. D. Drummond, *J. Psychopharmacol.* **2012**, *26*, 1512–1524; c) D. Perrone, F. Ardito, G. Giannatempo, M. Dioguardi, G. Troiano, L. Lo Russo, A. De Lillo, L. Laino, L. Lo Muzio, *Exp. Ther. Med.* **2015**, *10*, 1615–1623.
- [6] a) M. Mimeault, S. K. Batra, *Chin. Med.* **2011**, *6*, 31; b) C. Cheng, S. Peng, Z. Li, L. Zou, W. Liu, *RSC Adv.* **2017**, *7*, 25978–25986; c) L. Zhang, S. Man, H. Qiu, Z. Liu, M. Zhang, L. Ma, *Environ. Toxicol. Pharmacol.* **2016**, *48*, 31–38; d) M. M. Yallapu, M. Jaggi, S. C. Chauhan, *Colloids Surf. B* **2010**, *79*, 113–125; e) J. Liu, S. Chen, L. Song, S. Guo, S. Hunag, *Curr. Pharm. Des.* **2013**, *19*, 1974–1993.
- [7] K. K. Laali, B. M. Rathman, S. D. Bunge, X. Qi, G. L. Borosky, *J. Fluorine Chem.* **2016**, *191*, 29–41.
- [8] K. K. Laali, W. J. Greve, S. J. Correa-Smits, A. T. Zwarycz, S. D. Bunge, G. L. Borosky, A. Manna, A. Paulus, A. Chanan-Khand, *J. Fluorine Chem.* **2018**, *206*, 82–98.
- [9] M. Martinez-Cifuentes, B. Weiss-Lopes, L. S. Santos, R. Araya-Maturana, *Curr. Topic. Med. Chem.* **2015**, *15*, 1663–1672.
- [10] T. Castanheiro, J. Suffert, M. Donnard, M. Gulea, *Chem. Soc. Rev.* **2016**, *45*, 494.
- [11] a) G. Malik, R. A. Swyka, V. K. Tiwari, X. Fei, G. A. Applegate, D. B. Berkowitz, *Chem. Sci.* **2017**, *8*, 8050–8060; b) D. Wu, J. Qiu, P. G. Karmaker, H. Yin, F.-X. Chen, *J. Org. Chem.* **2018**, *83*, 1576–1583.
- [12] K. K. Laali et al., unpublished results.
- [13] N. Iqbal, N. Iqbal, *Mol. Biol. Intell.* **2014**, *2014*, 852748.
- [14] K.-L. Tan, S.-B. Koh, R. P.-L. Ee, M. Khan, M.-L. Go, *ChemMedChem* **2012**, *7*, 1567–1579.
- [15] S. B. Wan, H. Yang, Z. Zhou, Q.-C. Cui, D. Chen, J. Kanwar, I. Mohammad, Q. P. Dou, T. H. Chan, *Int. J. Mol. Med.* **2010**, *26*, 447–455.
- [16] M. McTigue, B. W. Murray, J. H. Chen, Y.-L. Deng, J. Solowiej, R. S. Kania, *Proc. Natl. Acad. Sci. USA* **2012**, *109*, 18281–18289.
- [17] C. Zhang, W. Spevak, Y. Zhang, E. A. Burton, Y. Ma, G. Habets, J. Zhang, J. Lin, T. Ewing, B. Matusow, G. Tsang, A. Marimuthu, H. Cho, G. Wu, W. Wang, D. Fong, H. Nguyen, S. Shi, P. Womack, M. Nespi, R. Shellooe, H. Carias, B. Powell, E. Light, L. Sanftner, J. Walters, J. Tsai, B. L. West, G. Visor, H. Rezaei, P. S. Lin, K. Nolop, P. N. Ibrahim, P. Hirth, G. Bollag, *Nature* **2015**, *526*, 583–586.
- [18] A. J. Souers, J. D. Levenson, E. R. Boghaert, S. L. Ackler, N. D. Catron, J. Chen, B. D. Dayton, H. Ding, S. H. Enschede, W. J. Fairbrother, D. C. S. Huang, S. G. Hymowitz, S. Jin, S. L. Khaw, P. J. Kovar, L. T. Lam, J. Lee, H. L. Maecker, K. C. Marsh, K. D. Mason, M. J. Mitten, P. M. Nimmer, A. Oleksijew, C. H. Park, C.-M. Park, D. C. Phillips, A. W. Roberts, D. Sampath, J. F. Seymour, M. L. Smith, G. M. Sullivan, S. K. Tahir, C. Tse, M. D. Wendt, Y. Xiao, J. C. Xue, H. Zhang, R. A. Humerickhouse, S. H. Rosenberg, S. W. Elmore, *Nat. Med.* **2013**, *19*, 202–208.
- [19] a) A. D. Becke, *J. Chem. Phys.* **1993**, *98*, 5648–5652; b) C. Lee, W. Yang, R. G. Parr, *Phys. Rev. B* **1988**, *37*, 785–789; c) B. Miehlisch, A. Savin, H. Stoll, H. Preuss, *Chem. Phys. Lett.* **1989**, *157*, 200–206.
- [20] Gaussian 09, Revision E.01, M. J. Frisch, G. W. Trucks, H. B. Schlegel, G. E. Scuseria, M. A. Robb, J. R. Cheeseman, G. Scalmani, V. Barone, B. Menonucci, G. A. Petersson, H. Nakatsuji, M. Caricato, X. Li, H. P. Hratchian, A. F. Izmaylov, J. Bloino, G. Zheng, J. L. Sonnenberg, M. Hada, M. Ehara, K. Toyota, R. Fukuda, J. Hasegawa, M. Ishida, T. Nakajima, Y. Honda, O. Kitao, H. Nakai, T. Vreven, J. A. Montgomery, Jr., J. E. Peralta, F. Ogliaro, M. Bearpark, J. J. Heyd, E. Brothers, K. N. Kudin, V. N. Staroverov, R. Kobayashi, J. Normand, K. Raghavachari, A. Rendell, J. C. Burant, S. S. Iyengar, J. Tomasi, M. Cossi, N. Rega, J. M. Millam, M. Klene, J. E. Knox, J. B. Cross, V. Bakken, C. Adamo, J. Jaramillo, R. Gomperts, R. E. Stratmann, O. Yazyev, A. J. Austin, R. Cammi, C. Pomelli, J. W. Ochterski, R. L. Martin, K. Morokuma, V. G. Zakrzewski, G. A. Voth, P. Salvador, J. J. Dannenberg, S. Dapprich, A. D. Daniels, Ö. Farkas, J. B. Foresman, J. V. Ortiz, J. Cioslowski, D. J. Fox, Gaussian, Inc., Wallingford, CT, **2009**.
- [21] O. Trott, A. J. Olson, *J. Comput. Chem.* **2010**, *31*, 455–461.
- [22] K. Aertgeerts, R. Skene, J. Yano, B.-C. Sang, H. Zou, G. Snell, A. Jennings, K. Iwamoto, N. Habuka, A. Hirokawa, T. Ishikawa, T. Tanaka, H. Miki, Y. Ohta, S. J. Sogabe, *J. Biol. Chem.* **2011**, *286*, 18756–18765.
- [23] C. Blackburn, C. Barrett, J. L. Blank, F. J. Bruzzese, N. Bump, L. R. Dick, P. Fleming, K. Garcia, P. Hales, Z. Hu, M. Jones, J. X. Liu, D. S. Sappal, M. D. Sintchak, C. Tsu, K. M. Gigstad, *Bioorg. Med. Chem. Lett.* **2010**, *20*, 6581–6586.
- [24] K. S. Chitta, A. Paulus, S. Akhtar, K. Blake-Kuranz, T. R. Caulfield, A. J. Novak, S. M. Ansell, P. Advani, S. Ailawadhi, T. Sher, S. Linder, A. Chanan-Khan, *Br. J. Haematol.* **2015**, *169*, 377–390.
- [25] a) A. Paulus, S. Akhtar, H. Yousaf, S. M. Paulus, Y. Bashir, T. R. Caulfield, M. Kuranz-Blake, K. Chitta, X. Wang, Y. Asmann, R. Hudec, W. Springer, S. Ailawadhi, A. Chanan-Khan, *Blood Cancer J.* **2017**, *7*, e565; b) A. Paulus, S. Akhtar, T. Caulfield, K. Samuel, H. Yousaf, Y. Bashir, Y. S. Paulus, D. Tran, R. Hudec, D. Cogen, L. Jiang, B. Edenfield, A. Novak, S. Ansell, T. Witzig, P. Martin, M. Coleman, V. Roy, S. Ailawadhi, K. Chitta, S. Linder, A. Chanan-Khan, *Blood Cancer J.* **2016**, *6*, e492.

Manuscript received: May 11, 2018

Revised manuscript received: June 27, 2018

Version of record online: August 5, 2018